Noncollinear magnetism in the high-pressure hcp phase of iron

Raquel Lizárraga,[1,2] Lars Nordström,[3] Olle Eriksson,[3] and John Wills[2]
[1]*Instituto de Física, Facultad de Ciencias, Universidad Austral de Chile, Casilla 567, Valdivia, Chile*
[2]*Los Alamos National Laboratory, Los Alamos, New Mexico 87545, USA*
[3]*Department of Physics and Materials Science, Ångström Laboratory, Uppsala University, Box 530, 751 21 Uppsala, Sweden*
(Received 1 February 2008; revised manuscript received 10 June 2008; published 13 August 2008)

The magnetic structure of iron in its high-pressure hcp phase has been investigated with the full-potential augmented plane wave with local orbitals method that allows for noncollinear magnetism. In our study we consider different spin spiral structures and three antiferromagnetic configurations that have been previously discussed in the literature. We found that some of the magnetic structures are only metastable, and that a nonsymmetric incommensurate spin spiral state with wave vector $\mathbf{q}=(0.56,0.22,0)2\pi/a$ and two different antiferromagnetic structures are the most stable ones being almost degenerate around the equilibrium volume. These magnetic structures ought to exist in the pressure range where hcp iron becomes stable.

DOI: 10.1103/PhysRevB.78.064410 PACS number(s): 75.30.Fv, 75.50.Bb, 74.25.Ha

I. INTRODUCTION

Recently, Shimizu *et al.*[1] reported superconductivity (SC) below 2 K in the high-pressure hexagonal close-packed (hcp) phase of iron. The superconducting pressure range was found to be between 15 and 30 GPa ($66<V<72$ a.u.^{3}/atom). This finding is of course surprising since conventional SC is incompatible with even a small amount of magnetic impurities. Iron, the most common ferromagnet, orders ferromagnetically at ambient conditions in the body-centered-cubic structure. When applying pressure ($\sim$13 GPa) iron undergoes a phase transition to the hcp structure which is believed to be a nonmagnetic phase.[2] However, even if true long-range magnetic order is not established, the strong magnetic fluctuations present in materials close to magnetic phase transitions are known to suppress conventional SC. Hence, the origin of the SC in iron is being extensively debated.[3,4]

Spin fluctuations have been discussed before[5,6] as mediators of SC in nearly magnetic materials, the so-called unconventional SC. By means of first-principles calculations, Mazin *et al.*[4] argued that the onset of SC in hcp iron can be explained by the conventional phonon mechanism[7,8] but not its sudden disappearance at pressures greater than 30 GPa. They concluded that magnetic fluctuations may play an important role in the superconducting phase of iron.

Total-energy calculations, based on density-functional theory (DFT),[9,10] showed that two antiferromagnetic (AFM) structures (see Fig. 1) are lower in energy than that of the nonmagnetic configuration at elevated pressures in the hcp phase of Fe. Furthermore, by allowing for magnetism, a better agreement between the calculated and experimental equation of state and elastic constants was obtained compared to the nonmagnetic quantities. A first-principles-based tight-binding total-energy model[11] was used to investigate noncollinear spin configurations and these calculations were compared to the two AFM structures, previously considered in Ref. 9. One of the AFM structures resulted to be more stable than the noncollinear states for pressures above 13 GPa.

DFT calculations of the temperature-dependent static paramagnetic spin susceptibility were performed for the high-pressure phase of iron.[12] It showed that there are strong magnetic fluctuations in the hcp phase, consistent with the conjecture in Ref. 4. This study found that the dominant fluctuations are incommensurate and antiferromagnetic, characterized by the wave vector $(0.56,0.22,0)2\pi/a$. At low temperature, they result in an ordered spin spiral state. Recent calculations[13] show that interatomic pair exchange interactions favor antiferromagnetic interplane stacking of the basal hcp planes. At the same time, nearest-neighbor in-plane exchange interaction parameters are also strongly antiferromagnetic. This should lead to magnetic frustration in the planar triangular lattice of hcp Fe. In contrast to these theoretical predictions, Mössbauer measurements[14–16] and x-ray magnetic circular dichroism experiments[17,18] on hcp iron have found no evidence of long-range magnetic order.

We present here full-potential calculations for several noncollinear structures such as spin spirals (SSs), the two AFM structures shown in Fig. 1, and the ferromagnetic (FM) configuration. In addition we have performed calculations for the nonsymmetric spin spiral with wave vector $\mathbf{q}=(0.56,0.22,0)2\pi/a$ and a third AFM configuration (AFM III) characterized by the wave vector $\mathbf{q}=(1/\sqrt{3},1/3,0)2\pi/a$ as suggested by the susceptibility calculations in Ref. 12. In that study, the AFM (III) structure turned out to be more stable than the AFM (I) and AFM (II) structures; however, a maximal peak in the spin susceptibility was obtained for the SS with $\mathbf{q}=(0.56,0.22,0)2\pi/a$. Our present investigation has been motivated by the theoretical evidence of magnetism, the prediction of an incommensurate magnetic structure,[4,12] and its possible relation to the unconventional SC in hcp iron.

II. METHOD

In this study the full-potential all-electron augmented plane wave with local orbitals method[19,20] has been utilized within the generalized gradient approximation (GGA).[21] This approach has been extensively employed in studies of noncollinear systems, e.g., fcc iron[20,22] and the rare earths.[23,24] This method does not impose any restrictions to the shape of the magnetization density and therefore it allows for intra-noncollinearity as well as internoncollinearity. It also incor-

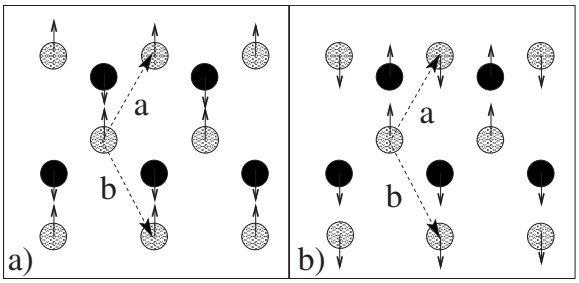

FIG. 1. The AFM structures denoted by I and II in Ref. 9 are shown in the (a) left and (b) right panels of the figure, respectively. The gray balls are in the *ab* plane of the hexagonal structure ($z=1/4$) and the darker balls lie at $z=3/4$. The AFM (I) consists of ferromagnetically ordered planes, perpendicular to the z axis, which alternate the direction of the spin. In the AFM (II) the planes are perpendicular to the x axis.

porates the symmetries of the SS (Ref. 23) in order to accurately calculate the total energies for various magnetic states in hcp Fe. From careful convergence tests with respect to the Brillouin-zone (BZ) sampling and the size of the basis set, we have determined that it is necessary to use a basis set cutoff corresponding to a largest reciprocal space lattice vector of 4.8 a.u.$^{-1}$ and a k-point mesh of $12\times12\times10$.

III. RESULTS AND DISCUSSION

In the present investigation we performed calculations for three values of the hcp structural parameter $c/a=1.58$, 1.59, and 1.60. In the following we will focus on the results for $c/a=1.58$. In Fig. 2 we display the calculated atomic magnetic moments for the two AFM configurations described in Fig. 1, the AFM (III) characterized by the wave vector $\mathbf{q}=(1/\sqrt{3},1/3,0)2\pi/a$, the nonsymmetric SS $\mathbf{q}=(0.56,0.22,0)2\pi/a$, a SS with $\mathbf{q}=(0.68,0.06,0)2\pi/a$, and the ferromagnetic state. The results for the two antiferromagnetic and ferromagnetic states agree very well with those obtained in Ref. 10, which is an erratum of Ref. 9. The ferromagnetic state shown in Fig. 2 corresponds to the high-spin solution and the magnetic moment has a maximum value of $2.72\mu_B$/atom at a volume of 90 a.u.^{3}/atom. The AFM (I) phase exists only for volumes larger than 72 a.u.^{3}/atom. The AFM (II), (III), and the nonsymmetric SS have almost the same atomic magnetic moment in the range of volumes of 60–90 a.u.^{3} Magnetic solutions do not seem to exist for volumes smaller than 60 a.u.^{3}/atom which corresponds to a pressure of ~65.8 GPa.

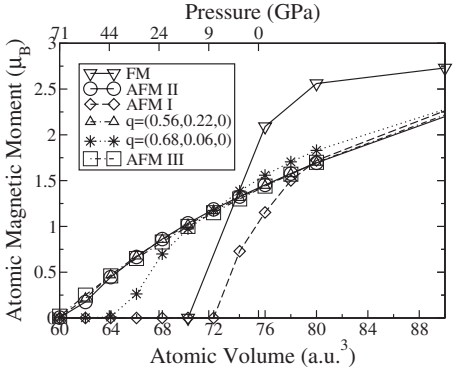

FIG. 2. Calculated atomic magnetic moments as a function of the atomic volume for the AFM (I), (II), and (III) configurations, the nonsymmetric SS with $\mathbf{q}=(0.56,0.22,0)2\pi/a$ and $\mathbf{q}=(0.68,0.06,0)2\pi/a$ and the high-spin ferromagnetic state. The scale in the upper x axis shows the values of the pressure for the respective atomic volumes as obtained in Ref. 25 by a third-order finite strain fit to the hydrostatic data for the hcp phase of Fe and it is only included here as a reference.

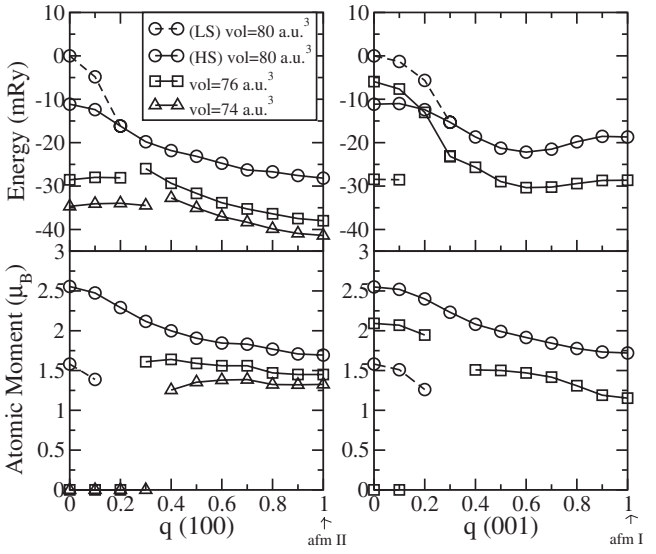

FIG. 3. In the upper panels the calculated total energies per atom of hcp Fe for volumes $V=74$, 76, and 80 a.u.^{3}/atom are plotted as a function of the wave vector $\mathbf{q}$ along two directions of the BZ, [100] (left panel) and [001] (right panel). The arrows indicate the AFM structures, I and II, described in Fig. 1. In the lower panels, the calculated atomic magnetic moments as a function of the wave vector $\mathbf{q}$ along the same two directions as in the upper panels are shown. The low-spin solution is shown by a dashed line.

We investigated SS solutions along two directions of the hexagonal hcp BZ, [100] and [001]. In the upper panels of Fig. 3, the calculated total energies of hcp Fe for several volumes are plotted as a function of the wave vector $\mathbf{q}$ along [100] (left panel) and [001] (right panel). We have chosen to show in this figure volumes around the zero-pressure volume of the hcp phase that was estimated by extrapolation of experimental data to be 75.4 a.u.^{3}/atom.[25,26] It is well known that iron in the fcc structure possesses the so-called high- and low-spin ferromagnetic states. Here, we also found ferromagnetic high-spin (full line) and low-spin (dashed line) states in hcp Fe for $V=80$ a.u.^{3} The AFM (I) configuration is represented by a wave vector $\mathbf{q}=(0,0,1)2\pi/c$ (shown with an arrow, right panel in Fig. 3) and consists of ferromagnetically ordered planes perpendicular to the z axis that alternate the direction of spin. In the AFM (II) phase, these planes are perpendicular to the x axis (see Fig. 1) and the magnetic structure corresponds to a wave vector $\mathbf{q}=(1,0,0)2\pi/a$.

We can see in the right upper panel of Fig. 3 that along the [001] direction there is a minimum at $\mathbf{q}\sim(0,0,0.6)2\pi/c$ which represents a SS where the parallel

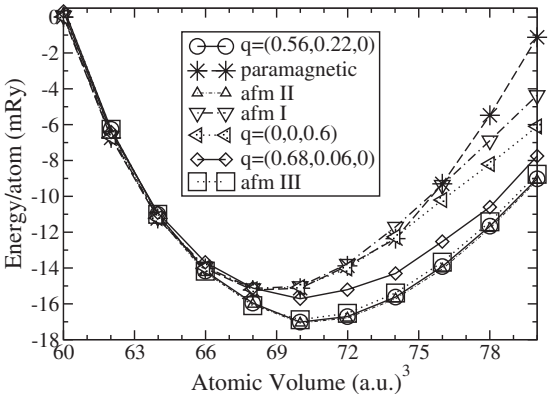

FIG. 4. The calculated total energy of hcp Fe in the SS state with $\mathbf{q}=(0.56,0.22,0)2\pi/a$ (circles), paramagnetic (stars), AFM (III) (squares), AFM (II) (up triangles), AFM (I) (down triangles), the SS state with $\mathbf{q}=(0,0,0.6)2\pi/c$ (left triangles), and a SS state with $\mathbf{q}=(0.68,0.06,0)$ (diamonds) are plotted as a function of the atomic volume. The zero of the energy was chosen to be the energy of the paramagnetic state at $V=60$ a.u.^{3}.

spins within a plane are rotating around the hexagonal axis with an angle $\phi=qc=0.62\pi\sim 216°$. The SS characterized by this $\mathbf{q}$ vector is then more stable than the AFM (I) structure for all volumes considered here. As the atomic volume becomes smaller this minimum gradually disappears. The low-spin FM solution also tends to die out and become nonmagnetic. For volumes smaller than 76 a.u.^{3}/atom, small $\mathbf{q}$ wave-vector states, i.e., $\mathbf{q}\sim 0$, along the [001] direction do not exist. However, the AFM (II) configuration along the [100] direction (shown by an arrow, left panel) is always the most stable state for all volumes. Steinle-Neumann *et al.*[11] investigated noncollinear configurations by using a tight-binding total-energy model and their results showed that the AFM (II) structure is more stable than the noncollinear structures studied by them. This is consistent with our findings although the noncollinear configurations considered by Steinle-Neumann *et al.*[11] are not the same noncollinear structures presented in this study.

In the lower panels of Fig. 3, we show the magnetic moments for several volumes along the same directions in the BZ as in the upper panels. For the largest atomic volume considered ($V=80$ a.u.^{3}), the high-spin and low-spin atomic magnetic moments are $2.55\mu_B$ and $1.58\mu_B$, respectively. The low-spin moment becomes zero for $V<76$ a.u.^{3} along the [001] and [100] directions.

In Fig. 4 the calculated total energies of hcp Fe in the AFM (II) (up triangles), AFM (I) (down triangles), and AFM (III) (squares), the nonsymmetric SS with $\mathbf{q}=(0.56,0.22,0)2\pi/a$ (circles), the SS with $\mathbf{q}=(0.68,0.06,0)2\pi/a$ (diamonds), the SS with $\mathbf{q}=(0,0,0.6)2\pi/c$ (left triangles), and the paramagnetic state (stars) are plotted as a function of the atomic volume. The paramagnetic curve has a minimum at 68.87 a.u.^{3}/atom and agrees well with calculations in Ref. 9. In this figure we can see that already for atomic volumes larger than 66 a.u.^{3}, corresponding to a pressure of $\sim$27.8 GPa,[25,26] magnetic solutions have lower energies than the paramagnetic one. The AFM (II), (III), and the nonsymmetric SS with $\mathbf{q}=(0.56,0.22,0)2\pi/a$ appear to be almost degenerate in the whole range of studied volumes with equilibrium volumes 70.64, 70.4, and 70.62 a.u.^{3}, respectively. At the equilibrium volume, the AFM (II) configuration is only $\sim$0.1 and $\sim$0.2 mRy lower in energy than the nonsymmetric SS and the AFM (III), respectively. The paramagnetic spin susceptibility calculations in Ref. 12 suggested that the most stable magnetic structure was the SS with $\mathbf{q}=(0.56,0.22,0)2\pi/a$, followed by the AFM (III) and the AFM (II) in ascending order. However, the present total-energy calculations show that these structures are indeed much closer in energy, almost degenerate. The spin susceptibility calculations were performed using the atomic sphere approximation that might produce different results[27] than a full-potential code when the energy differences between magnetic structures are very small and hence the accuracy required to distinguish between them is high.

TABLE I. Equilibrium volumes and energy differences for the AFM (I), (II), and (III), $\mathbf{q}=(0.56,0.22,0)2\pi/a$, $\mathbf{q}=(0,0,0.6)2\pi/c$, $\mathbf{q}=(0.68,0.06,0)2\pi/a$, and the paramagnetic state. The energy of the paramagnetic state of the present calculations at $V=60$ a.u.^{3}, $E=-2546.2719$ Ry, was used as reference to compute the energy differences (see Fig. 4).

	Energy difference (mRy)	Volume (a.u.^{3}/atom)
GGA paramagnetic	−15.24	68.87
GGA AFM (I)	−15.14	68.85
GGA AFM (II)	−17.00	70.64
GGA AFM (III)	−16.8	70.4
GGA $\mathbf{q}=(0.56,0.22,0)$	−16.93	70.62
GGA $\mathbf{q}=(0,0,0.6)$	−15.18	68.88
GGA $\mathbf{q}=(0,68,0.06,0)$	−15.62	70.1

The AFM (I) phase and the SS with $\mathbf{q}=(0,0,0.6)2\pi/c$ exist only for volumes greater than 72 a.u.^{3}, where they both have lower energies than the nonmagnetic state. We have listed in Table I the equilibrium volume and the energy for the equilibrium volume with respect to the energy of the paramagnetic state at $V=60$ a.u.^{3} for the paramagnetic, the AFM (III), (II) and (I), and some SS states. The equilibrium volume for the AFM (I) and AFM (II) configuration compare reasonable well with the results of previous first-principles calculations.[9–11] Our results also concur with the statement in Ref. 9 that magnetic solutions are more stable than the paramagnetic state. We would like to point out here that magnetic structures appear to be more stable than the paramagnetic state for volumes larger than 66 a.u.^{3}, which corresponds to a pressure of the order of $\sim$28 GPa; around the same pressure in which the superconducting state vanishes (30 GPa). In particular, the noncollinear spin spiral with $\mathbf{q}=(0.56,0.22,0)2\pi/a$ was shown[12] to be related to Fermi-surface features; a fact that has been discussed before[28] as a necessary condition for noncollinear magnetism to exist. All these findings lead us to speculate that strong magnetic fluctuations may indeed be responsible for the superconducting state in hcp Fe and a noncollinear structure may be the magnetic ground state for hcp Fe.

IV. CONCLUSIONS

We have investigated the magnetic structure of hcp Fe under pressure by performing first-principles total-energy calculations. Spin spirals were considered in this study along two symmetry directions of the BZ, [001] and [100]. The end points of the symmetry lines corresponds to the two antiferromagnetic structures (I and II) that have previously been reported by theory to exist in the hcp phase of Fe. A nonsymmetric spin spiral with wave vector $(0.56,0.22,0)2\pi/a$ was also studied. Calculations of the temperature-dependent susceptibility in Ref. 12 suggest that this incommensurate structure is a good candidate to be the magnetic structure of hcp Fe. Our results show three, almost degenerate states, to have the lowest energy. The AFM (III), (II), and a nonsymmetric spin spiral with $\mathbf{q}=(0.56,0.22,0)2\pi/a$ are the most stable structures with a magnetic moment of $\sim 1\mu_B$/atom and an equilibrium volume of 70.6 a.u.[3]

ACKNOWLEDGMENTS

Support from the Swedish Research Council (VR) and the Swedish Foundation for Strategic Research (SSF) are acknowledged. We are also thankful for the support from the Swedish National Allocation Committee (SNAC). R.L. would like to acknowledge support from DID-UACh: Project No. S-200851 and CONICYT (Chile) under Grant ACT24/2006.

[1] K. Shimizu, T. Kimura, S. Furomoto, K. Takeda, K. Kontani, Y. Onuki, and K. Amaya, Nature (London) **412**, 316 (2001).
[2] R. D. Taylor, M. P. Pasternak, and R. Jeanloz, J. Appl. Phys. **69**, 6126 (1991).
[3] T. Jarlborg, Phys. Lett. A **300**, 518 (2002).
[4] I. I. Mazin, D. A. Papaconstantopoulos, and M. J. Mehl, Phys. Rev. B **65**, 100511(R) (2002).
[5] D. Fay and J. Appel, Phys. Rev. B **22**, 3173 (1980).
[6] I. I. Mazin and D. J. Singh, Phys. Rev. Lett. **79**, 733 (1997).
[7] J. Bardeen, L. N. Cooper, and J. R. Schrieffer, Phys. Rev. **106**, 162 (1957).
[8] J. Bardeen, L. N. Cooper, and J. R. Schrieffer, Phys. Rev. **108**, 1175 (1957).
[9] G. Steinle-Neumann, L. Stixrude, and R. E. Cohen, Phys. Rev. B **60**, 791 (1999).
[10] G. Steinle-Neumann, L. Stixrude, and R. E. Cohen, Phys. Rev. B **69**, 219903(E) (2004).
[11] G. Steinle-Neumann, R. E. Cohen, and L. Stixrude, J. Phys.: Condens. Matter **16**, S1109 (2004).
[12] V. Thakor, J. B. Staunton, J. Poulter, S. Ostanin, B. Ginatempo, and E. Bruno, Phys. Rev. B **67**, 180405(R) (2003).
[13] S. Khmelevskyi, A. V. Ruban, and P. Mohn, Physica C **460-462**, 647 (2007).
[14] M. F. Nicol and G. Jura, Science **141**, 1035 (1963).
[15] R. D. Taylor, G. Cort, and J. O. Willis, J. Appl. Phys. **53**, 8199 (1982).
[16] A. B. Papandrew, M. S. Lucas, R. Stevens, I. Halevy, B. Fultz, M. Y. Hu, P. Chow, R. E. Cohen, and M. Somayazulu, Phys. Rev. Lett. **97**, 087202 (2006).
[17] V. Iota, J.-H. Park Klepeis, and Choong-Shik Yoo, Appl. Phys. Lett. **90**, 042505, (2007).
[18] N. Ishimatsu, H. Maruyama, N. Kawamura, M. Suzuki, Y. Ohishi, and O. Shimomura, J. Phys. Soc. Jpn. **76**, 064703 (2007).
[19] E. Sjöstedt, L. Nordström, and D. J. Singh, Solid State Commun. **114**, 15 (2000).
[20] E. Sjöstedt and L. Nordström, Phys. Rev. B **66**, 014447 (2002).
[21] J. P. Perdew and Y. Wang, Phys. Rev. B **46**, 12947 (1992).
[22] R. Lizárraga, E. Sjöstedt, and L. Nordström (unpublished).
[23] L. Nordström and A. Mavromaras, Europhys. Lett. **49**, 775 (2000).
[24] R. Lizárraga, A. Bergman, T. Björkman, H. P. Liu, Y. Andersson, T. Gustafsson, A. G. Kuchin, A. S. Ermolenko, L. Nordström, and O. Eriksson, Phys. Rev. B **74**, 094419 (2006).
[25] A. P. Jephcoat, H. K. Mao, and P. Bell, J. Geophys. Res. **91**, 4677 (1986).
[26] H. K. Mao, Y. Wu, L. C. Chen, J. F. Shu, and A. P. Jephocoat, J. Geophys. Res. **95**, 21737 (1990).
[27] R. Lizárraga, S. Ronneteg, R. Berger, A. Bergman, O. Eriksson, and L. Nordström, Phys. Rev. B **70**, 024407 (2004).
[28] R. Lizárraga, L. Nordström, L. Bergqvist, A. Bergman, E. Sjöstedt, P. Mohn, and O. Eriksson, Phys. Rev. Lett. **93**, 107205 (2004).